

and, second, the muzzle properties change continuously as the weapon empties. While the present model cannot treat the actual flow, estimates are possible of the global influence of these effects. For the M109A1 howitzer, the decay in exit properties is given in Table 1.

The growth and decay of the inviscid core are approximated using a one-dimensional, time-dependent calculation⁴ to describe the flow along the axis of symmetry coupled to experimental results¹ to define the off-axis shock structure. The data describe the trajectory of the triple point marking the junction of the intercepting shock and Mach disk, Fig. 3. Superimposed on this figure are computed contours of relative mass flux showing that during the initial growth of the plume nearly all of the exhaust mass is processed through the Mach disk; whereas, later in the emptying cycle, the influence of the Mach disk is greatly diminished.

Using the computed Mach disk velocity, a relative flow Mach number and shock jump conditions are evaluated. For each time considered, the mixture temperatures are determined. The maximum value of this parameter over the interval $0.2 < r < 0.8$ is shown in Fig. 4. At the beginning, the temperature is very high due to the large mass flow through the Mach disk. As the growth of the plume continues, the mixture temperatures monotonically decay and at later times are dominated by the muzzle exit properties and decreasing mass flow through the Mach disk. The calculation predicts highest probability of ignition early in the exhaust cycle; a conclusion supported in part by observations of actual firings showing ignition soon after shot ejection.

Summary and Conclusions

A simple model of ignition in gun exhaust plumes is presented. While it treats the gasdynamics and chemistry in an approximate fashion, the technique can be easily coupled to existing inviscid analyses of muzzle flow and used to point out qualitative variations in flash processes. Calculations clearly display the strong influence of muzzle devices and time dependence upon the ignition process.

References

- ¹Schmidt, E. and Shear, D., "Optical Measurements of Muzzle Blast," *AIAA Journal*, Vol. 13, Aug. 1975, pp. 1086-1091.
- ²Carfagno, S., *Handbook on Gun Flash*, The Franklin Institute, Philadelphia, Pa., 1961.
- ³Yousefian, V., "Muzzle Flash Onset," Aerodyne Research, Inc., Bedford, Mass., ARI-RR-161.1, May 1979.
- ⁴Erdos, J. and DelGuidice, P., "Calculation of Muzzle Blast Flowfields," *AIAA Journal*, Vol. 13, Aug. 1975, pp. 1048-1055.

Adhesive Bonded Orthotropic Structures with a Part-Through Crack

C. S. Hong* and H. S. Ro†
Korea Advanced Institute of Science
and Technology, Seoul, Korea

Introduction

IN recent years, considerable attention has been paid to the problem of adhesive bonded joints, as a result of growing interest in the damage-tolerant design of aircraft structures.

Received April 24, 1981; revision received Jan. 19, 1983. Copyright © American Institute of Aeronautics and Astronautics, Inc., 1983. All rights reserved.

*Associate Professor, Dept. of Aeronautical Engineering. Member AIAA.

†Graduate Student, Dept. of Mechanical Engineering; presently with Samsung Heavy Industries Co., Ltd., Changwon, Korea.

Composite materials, due to their high strength-to-weight ratio, are being widely used in aircraft structures with adhesive bonded joints. Structural reliability is one of the main concerns of analytical and experimental research.

Several studies have been made on the problem of adhesively bonded structures.¹⁻⁶ Keer et al.¹ solved the problem of a cracked plate by using Fourier transform techniques and reduced it to a solution by integral equation. Arin and Erdogan²⁻⁴ used a complex variable formulation to equations. Ko⁵ analyzed an orthotropic sandwich plate containing a part-through crack subjected to in-plane mixed mode tractions. He formulated the problem and reduced it to a set of integral equations, but did not obtain the numerical solution of the equations. Ratwani⁶ outlined finite element and mathematical methods of analysis for a two-isotropically, adhesively bonded structure. The purpose of this Note is to extend Ratwani's isotropic structure solution to adhesive bonded orthotropic structures with a part-through crack. Some numerical results for stress intensity factors are presented for various values of crack length and adhesive thickness.

Formulation of the Problem

The orthotropic plate with a crack and a sound orthotropic plate are of the same width, and are assumed infinitely wide. Consider the adhesively bonded structure of Fig. 1a, consisting of two plates with thickness h_1 and h_2 , respectively, and bonded through an adhesive layer of constant thickness h_a . The plate is subjected to forces T_x and T_y per unit length of the plate. Plate 1 is assumed to have a through-crack and a debond in the adhesive around the crack.

In Fig. 1a, the size of the debond is shown to be the same as the length of the crack. If the initial debonding size in the adhesive is large, it is possible that the crack length will be shorter than the debond. However, this problem can still be formulated in a similar manner. The analysis of the adhesively bonded structure in Fig. 1a will be based on the following assumptions. The plate and the adhesive layer are homogeneous and linearly elastic. The thickness of the adhesive is small compared to the thickness of the adherends;

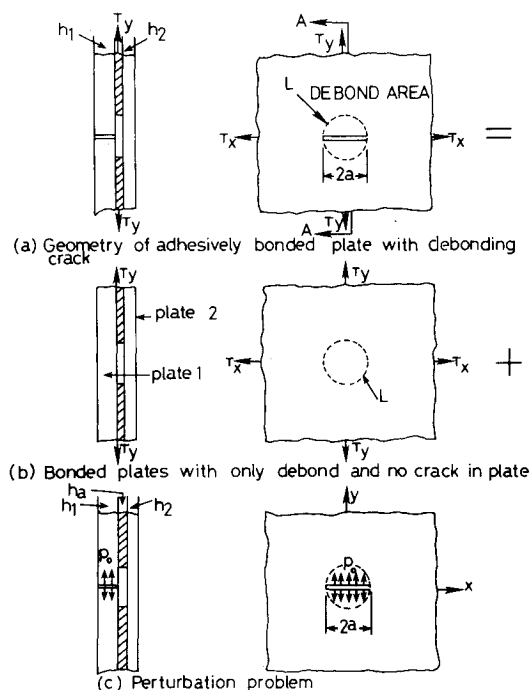


Fig. 1 Superposition technique for an adhesively bonded plate with a debonding area.

hence the adhesive may be treated as shear spring. The surface shear transmitted through the adhesive acts as a body force.

Let u_1, v_1 and u_2, v_2 be x, y components of the in-plane displacement vectors in plates 1 and 2, respectively, and τ_x and τ_y be components of shear stress acting on the adhesive. The above assumption yields the following continuity conditions:

$$u_1 - u_2 = (h_a/G_a)\tau_x; \quad v_1 - v_2 = (h_a/G_a)\tau_y \quad (1)$$

where G_a is shear modulus of the adhesive and h_a is adhesive thickness. The body forces acting on plates 1 and 2 are given by

$$\begin{aligned} X_1 &= -(\tau_x/h_1), & Y_1 &= -(\tau_y/h_1) \\ X_2 &= -(\tau_x/h_2), & Y_2 &= -(\tau_y/h_2) \end{aligned} \quad (2)$$

where h_1 and h_2 are the thickness of plates 1 and 2, respectively.

The equilibrium conditions in the x and y directions and the continuity of displacement in the problem of Fig. 1b gives the crack surface stress P_0 applied to the crack surface in the perturbation problem of Fig. 1c. The stress P_0 is equal to $T_1 y/h_1$ and is given by

$$P_0 = (a_1 T_x + a_2 T_y)/a_3 \quad (3)$$

where

$$\begin{aligned} a_1 &= \frac{h_2}{h_1} \left[\frac{E_{2x}}{h_1 E_{1x} + h_2 E_{2x}} - \frac{\nu_{1y} E_{2y}}{\nu_{2y} h_1 E_{1y} + \nu_{1y} h_2 E_{2y}} \right] \\ a_2 &= \frac{\nu_{2x} E_{1x}}{h_1 E_{1x} + h_2 E_{2x}} - \frac{E_{1y}}{\nu_{2y} h_1 E_{1y} + \nu_{1y} h_2 E_{2y}} \\ a_3 &= \frac{\nu_{2x} h_1 E_{1x} + \nu_{1x} h_2 E_{2x}}{h_1 E_{1x} + h_2 E_{2x}} - \frac{h_1 E_{1y} + h_2 E_{2y}}{\nu_{2y} h_1 E_{1y} + \nu_{1y} h_2 E_{2y}} \end{aligned} \quad (4)$$

where E and ν denote elastic moduli and Poisson's ratio, respectively. The first subscript denotes the plate and the second denotes the direction.

Displacements in an orthotropic plate can be written as follows:³

$$\begin{aligned} u &= 2\text{Re}[p_1 \phi_1(z_1) + p_2 \phi_2(z_2)] \\ v &= 2\text{Re}[q_1 \phi_1(z_1) + q_2 \phi_2(z_2)] \end{aligned} \quad (5)$$

where

$$P_k = \frac{1}{E_x} (\mu_k^2 - \nu_k), \quad q_k = \frac{1}{u_k E_y} (1 - \nu_y \mu_k^2), \quad k=1,2$$

Displacements in the cracked plate will consist of two components—one due to uniform applied pressure on the crack surface and the other due to body forces acting on the plate surface. Displacements due to uniform applied stress are given as follows:⁴

$$\begin{aligned} U_{11} &= P_0 \text{Re} \left[\frac{1}{\mu_1 - \mu_2} \{ p_1 \mu_2 (z_1 - \sqrt{z_1^2 - a^2}) \right. \\ &\quad \left. - p_2 \mu_1 (z_2 - \sqrt{z_2^2 - a^2}) \} \right] \\ V_{11} &= P_0 \text{Re} \left[\frac{1}{\mu_1 - \mu_2} \{ q_1 \mu_2 (z_1 - \sqrt{z_1^2 - a^2}) \right. \\ &\quad \left. - q_2 \mu_1 (z_2 - \sqrt{z_2^2 - a^2}) \} \right] \end{aligned} \quad (6)$$

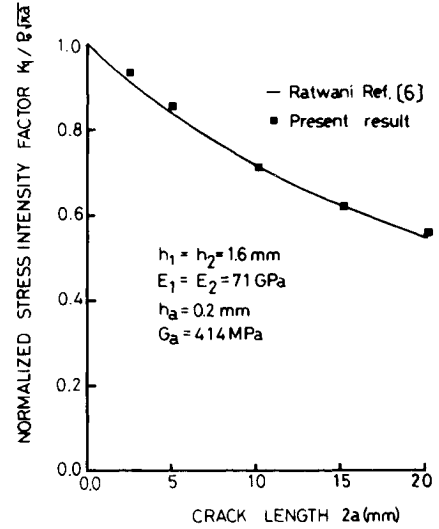


Fig. 2 Stress intensity factors for a two-isotropic ply, adhesively bonded structure.

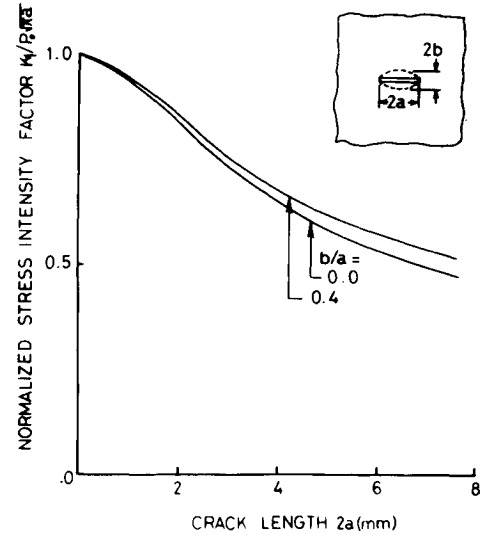


Fig. 3 Influence of debonding size on the stress intensity factors in a two-layer bonded structure.

Assuming that the body forces (X_1, Y_1) are a continuous function of (x_0, y_0) defined in region D, displacements in the cracked plate may be expressed as

$$\begin{aligned} U_{12}(x, y) &= \iint_D [H_{11}(x, y; x_0, y_0) X_1(x_0, y_0) \\ &\quad + H_{12}(x, y; x_0, y_0) Y_1(x_0, y_0)] dx_0 dy_0 \\ V_{12}(x, y) &= \iint_D [H_{21}(x, y; x_0, y_0) X_1(x_0, y_0) \\ &\quad + H_{22}(x, y; x_0, y_0) Y_1(x_0, y_0)] dx_0 dy_0 \end{aligned} \quad (7)$$

where kernels $H_{ij}(i, j=1, 2)$ are given by Green's functions. Therefore, total displacements in the cracked plate may be obtained as followings:

$$\begin{aligned} u_1(x, y) &= U_{11}(x, y) + U_{12}(x, y), \\ v_1(x, y) &= V_{11}(x, y) + V_{12}(x, y) \end{aligned} \quad (8)$$

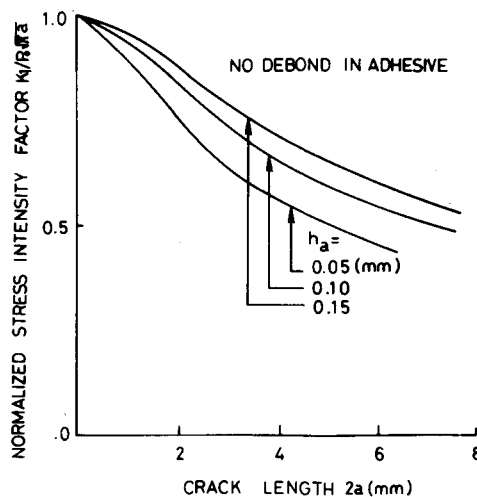


Fig. 4 Influence of adhesive thickness on the stress intensity factors in a two-layer, bonded structure.

In the problem considered here, the opening component K_I is determined by adding the effects of the crack surface pressure P_0 and the body forces X_I and Y_I . The stress intensity factor can be written as

$$\frac{K_I}{\sqrt{a}} + \frac{K_2/\sqrt{a}}{\mu_2} = P_0 + \iint_D [h_I(x_0, y_0) X_I(x_0, y_0) + h_2(x_0, y_0) Y_I(x_0, y_0)] dx_0 dy_0 \quad (9)$$

In the problem considered here, the shear component of the stress intensity factor K_2 is zero due to the symmetry in loading and geometry.

Numerical Examples

The system of integral equations given by Eq. (6) is the Fredholm type and may be solved by using the standard numerical techniques. In this case, it is done by dividing region D into smaller cells, and unknown functions τ_x and τ_y are assumed to be constant in each cell. Thus, using a numerical integration scheme, the integral equations are reduced to a system of algebraic equations. The kernels in the integral equations have logarithmic singularities, hence the singular part of the kernels is evaluated separately, in closed form. In the actual integration a telescopic grid is used. The cell size is kept small above the crack surface for a distance of about a half-crack length, as the shear stresses are high in this region and are maximum at the boundary of debond. The cell size is progressively increased. The debonded region is approximately represented by a straight line for integration purpose. The boundary of the domain of integration goes to infinity, hence the size of region D is restricted in numerical analysis such that the stress intensity factors are not appreciably affected.

The convergence of the solution also depends on the crack length. If $h_a G_a$ is very small or the half-crack length is large, the solution will not converge and the shear stresses will oscillate. This can be avoided by decreasing the cell size further and increasing the integration area.

Stress intensity factors for mode I (opening mode) and shear stress distribution on the adhesive layer were calculated. The program is fully capable of studying generally orthotropic plates and obtaining values of K_I and K_2 .

First, stress intensity factors for the isotropic plate were calculated to test the program in special case. The characteristic roots for an isotropic plate are equal for isotropic material, so the complex constant A_k becomes infinite. To avoid this computational problem with this program, the

characteristic roots $1.1i$ and $0.9i$ were used. These results are plotted in Fig. 2. These results agree well with the results of Ref. 6 within 6% discrepancy. In the problem of orthotropic plates, adherends and adhesive are boron-epoxy and epoxy, respectively, and their properties are: $E_{1x} = E_{2x} = 24$ GPa, $E_{1y} = E_{2y} = 223$ GPa, $\nu_{yx} = 0.23$, $G_{xy} = 8.4$ GPa, $h_1 = h_2 = 2.3$ mm, $G_a = 113.8$ MPa, and $h_a = 0.1$ mm. The influence of debonding size on the stress intensity factors for various crack lengths is shown in Fig. 3. These stress intensity factors have been obtained for no debond and elliptical debond. The end of the major axis of the debond is assumed to coincide with the leading edge of the crack. It is seen that an increase in debonding size increases the stress intensity factors due to less load transfer to the sound layer. The variation of the stress intensity factors with the crack length $2a$ for the various values of the adhesive thickness h_a is shown in Fig. 4.

Conclusions

A mathematical method is outlined to crack problems in adhesively bonded orthotropic structures. The mathematical method of analysis is very useful in analyzing crack problems in a two-orthotropic-ply, adhesively bonded structure; as it is in a two-isotropic-ply, adhesively bonded structure. A debond in the adhesive will cause less load transfer to the sound layer; hence an increase in the stress intensity factors. An increase in adhesive thickness, or a reduction in shear modulus, causes less load transfer to the sound layer, resulting in an increase in the stress intensity factors.

References

- Keer, L. M., Liu, C. T., and Mura, T., "Fracture Analysis of Adhesively Bonded Sheets," *Transactions of ASME, Journal of Applied Mechanics*, Vol. 43, Dec. 1976, pp. 652-656.
- Arin, K., "A Plate with a Crack Stiffened by a Partially Debonded Stringer," *Engineering Fracture Mechanics*, Vol. 6, 1974, pp. 133-140.
- Erdogan, F. and Arin, K., "A Sandwich Plate with a Part-Through and a Debonding Crack," *Engineering Fracture Mechanics*, Vol. 4, 1972, pp. 449-458.
- Arin, K., "Several Intact or Broken Stringers Attached to an Orthotropic Sheet with a Crack," *Engineering Fracture Mechanics*, Vol. 11, 1979, pp. 1-8.
- Ko, W. L., "An Orthotropic Sandwich Plate Containing a Part-Through Crack under Mixed Mode Deformation," *Engineering Fracture Mechanics*, Vol. 10, 1978, pp. 15-23.
- Ratwani, M. M., "Analysis of Cracked, Adhesively Bonded Laminated Structures," *AIAA Journal*, Vol. 17, Sept. 1979, pp. 988-994.

The Affine Equivalence of Local Stress and Displacement Distributions in Damaged Composites and Batdorf's Electric Analog

E. J. Brunelle*

Rensselaer Polytechnic Institute, Troy, New York

Nomenclature

a, b, c = analog device dimensions
 a_1, b_1, c_1 = composite solid dimensions

Received Dec. 15, 1982; revision submitted May 11, 1983. Copyright © 1983 by E. J. Brunelle. Published by the American Institute of Aeronautics and Astronautics, Inc., with permission.

*Associate Professor, Department of ME/AE/Mechanics (currently Professor, Air Force Institute of Technology, WPAFB, Ohio).